



Published in final edited form as:

Nature. ; 479(7371): 67–73. doi:10.1038/nature10567.

Melanopsin Signaling in Mammalian Iris and Retina

T. Xue^{1,3}, M. T. H. Do^{1,3,11}, A. Riccio⁷, Z. Jiang^{1,3}, J. Hsieh^{1,5}, H. C. Wang^{1,4}, S. L. Merbs², D. S. Welsbie², T. Yoshioka^{1,6}, P. Weissgerber⁸, S. Stolz⁸, V. Flockerzi⁸, M. Freichel⁸, M. I. Simon⁹, D. E. Clapham⁷, and K.-W. Yau^{1,2,3}

¹Solomon H. Snyder Department of Neuroscience, Johns Hopkins University School of Medicine, Baltimore, MD 21205, USA

²Department of Ophthalmology, Johns Hopkins University School of Medicine, Baltimore, MD 21205, USA

³Center for Sensory Biology, Johns Hopkins University School of Medicine, Baltimore, MD 21205, USA

⁴Neuroscience Graduate Program, Johns Hopkins University School of Medicine, Baltimore, MD 21205, USA

⁵BA/MS Concurrent Program in Neuroscience, Johns Hopkins University, Baltimore, MD 21238

⁶The Zanvyl Krieger Mind/Brain Institute, Johns Hopkins University, Baltimore, MD 21238

⁷Department of Cardiology, Children's Hospital Boston, Harvard Medical School, and Howard Hughes Medical Institute, Boston, MA 02115

⁸Institut für Experimentelle und Klinische Pharmakologie und Toxikologie, Universität des Saarlandes, Homburg/Saar, Germany

⁹Division of Biology, California Institute of Technology, Pasadena CA 91125

Users may view, print, copy, download and text and data- mine the content in such documents, for the purposes of academic research, subject always to the full Conditions of use: http://www.nature.com/authors/editorial_policies/license.html#terms

Address for Editorial Correspondence: Dr. King-Wai Yau, Room 905A Preclinical Teaching Building, Johns Hopkins University School of Medicine, 725 North Wolfe Street, Baltimore, MD 21205, USA, Tel: 410-955-1260, FAX: 410-955-1948, kwyau@mail.jhmi.edu. Correspondence and requests for materials should be addressed to T.X. (txue77@gmail.com) or K.-W.Y. (kwyau@mail.jhmi.edu).

¹¹ Present address: F.M. Kirby Neurobiology Center, Department of Neurology, Children's Hospital Boston and Harvard Medical School, Boston, MA 02115

Supplementary Information is linked to the online version of the paper at www.nature.com/nature.

Author Contributions. T.X., M.T.H.D. and K.-W.Y. designed the experiments. T.X. and M.T.H.D. did the isolated-eyeball experiments. T.X. carried out all muscle recordings and also *Trpcs*-KOs ipRGC recordings at 23°C (recordings at 35°C were by Z.J.), the mouse-optic-nerve transections, some of the *in situ* PLR measurements (the rest done by J.H.), some of the RT-PCR experiments on melanopsin (the rest done by H.C.W.), the tdTomato-fluorescence experiments, and the generation and maintenance of all double, triple and quadruple genetically-engineered mouse lines for this study. The recordings from ipRGCs of *Plcβ4*^{-/-} mice and their WT littermates were done by M.T.H.D. (23°C) and Z.J. (35°C). T.X., M.T.H.D. and J.H. designed the head-fixed, dual-PLR-recording instrument. H.C.W. and T.X. did the anterior-chamber measurements. H.C.W. did the immunocytochemistry and X-gal labeling. S.L.M. and D.W. did the surgery of transecting the optic nerve in anesthetized monkeys, and tested the PLR with T.X. and M.T.H.D. T.Y. participated in the monkey experiments. A.R. in D.E.C.'s laboratory made the *TRPC7*^{-/-} mouse line and did the associated characterization (retinal RT-PCR done by T.X.). P.W., S.S., V.F. and M.F. made the *TRPC5*^{-/-} line and did the associated characterization, and also provided the *Trpc4*^{-/-} and *Trpc4.5*^{-/-} lines. M.I.S. provided the *Plcβ4*^{-/-} line. T.X., M.T.H.D. and Z.J. analyzed the data with assistance from J.H., and, together with K.-W.Y., wrote the paper.

Reprints and permissions information is available at www.nature.com/reprints.

Abstract

Lower vertebrates have an intrinsically-photosensitive iris and thus a local pupillary light reflex (PLR). In contrast, it has been a dogma that the PLR in mammals generally requires neuronal circuitry connecting the eye and the brain. We report here that an intrinsic component of the PLR is actually widespread in nocturnal and crepuscular mammals. In mouse, this intrinsic PLR requires the visual pigment, melanopsin. It also requires PLC β 4, the vertebrate homolog of the *Drosophila* NorpA phospholipase C mediating rhabdomeric phototransduction. The *Plc β 4*^{-/-} genotype, besides removing the intrinsic PLR, also essentially eliminates the intrinsic light response of the M1-subtype of melanopsin-expressing, intrinsically-photosensitive retinal ganglion cells (M1-ipRGCs), by far the most photosensitive ipRGCs and with the largest responses. Ablating in mouse the expression of both TRPC6 and TRPC7, members of the TRP channel superfamily, likewise essentially eliminated the M1-ipRGC light response, but spared the intrinsic PLR. Thus, melanopsin signaling exists in both iris and retina, involving a PLC β 4-mediated pathway that nonetheless diverges in the two locations.

The discovery of ipRGCs has overturned the century-old belief that rods and cones are the only mammalian retinal photoreceptors¹⁻⁶. These ganglion-cell photoreceptors serve primarily non-image visual functions, with one being the PLR. For lower vertebrates such as fish, amphibian and bird, in addition to the neurally-driven PLR, the iris itself is capable of autonomous, light-induced constriction⁷⁻¹¹. For mammals, the PLR is thought to generally require neuronal circuitry through the brain, although sporadic reports^{7,12,13} and controversy exist of an intrinsic iridic photosensitivity in occasional species, including human. Even in lower vertebrates, the photopigment driving the intrinsic PLR remains unidentified. It has been suggested to be rhodopsin in amphibians and fish^{8,9}, and the non-opsin-based cryptochrome in chicken¹¹.

We have examined this unsettled question of an intrinsic PLR in mammals, and found the phenomenon to be surprisingly widespread. Moreover, the intrinsic PLR bears a close kinship to the ipRGCs in phototransduction.

Intrinsic PLR in mouse and other mammals

We found that bright light triggered a pupillary constriction in an intact eye freshly isolated from a dark-adapted pigmented mouse (Fig. 1a; 3 eyes; **Methods**). This photosensitivity disappeared within ~1 min after eye-isolation perhaps due to anoxia, with the pupil remaining constricted thereafter. This PLR persisted in a reduced preparation with just the eye's anterior chamber and iris^{8,11,12} under L-15 medium (Fig. 1b; 3 eyes; **Methods**), even after blocking any potential parasympathetic activity to the iris with 0.5% atropine; however, the PLR again faded after a few light trials.

The mammalian iris has three main tissue layers, all pigmented with melanin: an anterior fibrovascular stroma, a middle smooth-muscle layer consisting of the circumferential sphincter muscle at the pupil perimeter and the radial dilator muscle across the iris, and a posterior epithelium^{7,14}. In lower vertebrates, the sphincter muscle itself is thought to be the light-sensor^{7,14}. Accordingly, we reduced the mouse preparation further to the small ring of

sphincter muscle, and connected it to a μ Newton strain gauge for measuring isometric tension under oxygenated Ames solution^{9,10} (35–37°C; **Methods**). The isolated sphincter muscle gave a light-induced contractile force reproducibly for hours. A relatively dim flash elicited a transient increase in force that grew linearly with increasing flash intensity, i.e., proportional to flash intensity and with a constant waveform (Fig. 1c and inset, bottom; Supplementary Fig. S1). This flash-induced contraction reached a transient peak in ~ 1 s but decayed much more slowly, not dissimilar to the *in situ* ipRGC-driven PLR¹⁵. The response to an intense flash often showed a hump during its decay (Fig. 1c inset, top). Although the force elicited by a dim flash decayed to baseline in ~ 1 min, a second identical flash typically elicited a smaller response unless given in ~ 8 min after the first. Likewise, a near-saturated response to an intense flash decayed in ~ 1 min, but a ~ 15 -min delay was required for a second identical flash to elicit a comparable response. This light adaptation was also manifested during steady light as a relaxation of the force from a transient peak to a lower plateau level (Fig. 1d; 3 muscles). In contrast, acetylcholine-elicited contraction did not show this adaptation (Supplementary Fig. S2), suggesting that this adaptation resided in the photosignaling pathway upstream of the contractile mechanism.

The intrinsic PLR turns out to be widespread across nocturnal mammals (**Methods**). Albino mice showed the same phenomenon but their sphincter muscle was more photosensitive (not shown) presumably due to higher light transmission through the non-pigmented iris. Albino rat (Fig. 2a, left; 2 muscles; pigmented species not tested) and hamster (Fig. 2a, right; 3 muscles; pigmented, but with little iridic melanin in the pupillary margin) also tested positively, with sensitivities similar to the albino mouse but a much larger muscle force. Dog, cat, and rabbit (all pigmented) also showed an intrinsic PLR (2, 1, 3 muscles respectively), but with distinctly lower photosensitivity and force production; cat and rabbit required a light step instead of flash to elicit a detectable response (Fig. 2b). Although these three species are strictly speaking not nocturnal, they are crepuscular, i.e., active at dawn and dusk. One somewhat unusual species, Nile grass rat, has both diurnal and nocturnal tendencies¹⁶ but also tested positively (3 muscles, not shown). On the other hand, the response was absent for guinea pig (2), ground squirrel (4) and pig (2) (not shown). Ground squirrel is strongly diurnal, while guinea pig and pig are variably described as crepuscular or diurnal. None of four primate species tested showed this phenomenon, including rhesus monkey (Fig. 2b; diurnal, 7 muscles), marmoset (diurnal, 2), owl monkey (nocturnal, 4) and bush baby (nocturnal, 2) (latter three not shown). Thus, nocturnal/nocturnal-leaning sub-primate mammals tend to have an intrinsic PLR.

Involvement of melanopsin in mammalian intrinsic PLR

The action spectrum for the isolated mouse sphincter muscle (**Methods**) fit an A₁-pigment spectral template¹⁷ with λ_{\max} at 480 nm (Fig. 3a), suggesting melanopsin's involvement^{3–6}. Indeed, the melanopsin-knockout¹⁸ (*Opn4*^{-/-}) muscle gave no light response (Fig. 3b). By RT-PCR, we detected melanopsin mRNA in the isolated wild-type (WT) mouse iris (Fig. 3c; **Methods**). Immunostaining (in an albino background for viewing immunofluorescence) also suggested melanopsin's presence in the sphincter muscle of WT, but not *Opn4*^{-/-}, iris (Fig. 3d; **Methods**). A BAC-transgenic mouse expressing the fluorescent protein, tdTomato, under the melanopsin promoter¹⁵ (*Opn4:tdTomato*, bred into an albino background)

likewise showed fluorescence at least in the sphincter muscle (Fig 3e). For rat and hamster, their particularly robust sphincter-muscle photoresponses (see above) allowed characterization of the associated action spectra, which also fit a 480-nm spectral template (Supplementary Fig. S3). Strictly speaking, because melanopsin appears to be more widespread than in just the sphincter muscle (Fig. 3d), contraction is not necessarily initiated by just light absorbed in the muscle itself, but this is likely.

For mouse, we were able to rule out any significant role of rhodopsin or cryptochromes in the sphincter-muscle photosensitivity (see Introduction); namely, besides a null contractile phenotype of the *Opn4*^{-/-} muscle, the responses from *Rho*^{-/-} (rhodopsin knockout¹⁹) and *Cry1,2*^{-/-} (cryptochromes-1,2 double-knockout²⁰) mice appeared normal (Supplementary Fig. S4a). We did find by RT-PCR rhodopsin mRNA in the dissected mouse iris (not shown; see also Ref. 21), but its significance is unclear.

By RT-PCR, we found melanopsin mRNA in the iris of rhesus monkey (not shown) and baboon (also diurnal; Supplementary Fig. S5), but the melanin-pigmentation confounded confirmation by immunohistochemistry. Melanopsin's function in the primate iris is likewise unclear because there is no intrinsic PLR.

Phototransduction mechanism underlying intrinsic PLR

Melanopsin shows a phylogenetic kinship to invertebrate rhabdomeric visual pigments²², thus possibly sharing a common phospholipase C (PLC)-mediated phototransduction pathway (see Ref. 23 for review). Moreover, PLC typically mediates membrane-receptor signaling in smooth muscles^{24,25}. Indeed, the sphincter muscle from *Plcβ4*^{-/-} mice²⁶ was practically unresponsive to light (Fig. 4a; 5 muscles). Sometimes, we observed a tiny response that disappeared after several stimuli (red trace in Fig 4b, top; dim flash; 3 out of 5 muscles), unlike the much larger and persistent WT response (black trace in Fig 4b, top; dim flash). This small response could be mediated by a different PLCβ isoform or another, minor pathway. The *Plcβ4*^{-/-} phenotype was not due to a defective contractile apparatus, because acetylcholine still elicited strong contraction via muscarinic receptors on the muscle¹⁴ (Fig. 4b, bottom). PLCβ4 is the closest vertebrate homolog²⁶ of the *Drosophila* PLC (NorpA) mediating phototransduction in rhabdomeric photoreceptors²³. Bath-applied U71322, a PLC-inhibitor, did not block the light-induced contraction of the WT sphincter muscle (not shown), but this may reflect poor drug penetration into the tissue (see below).

Smooth-muscle contraction often involves intracellular Ca²⁺ release (triggered by PLC via IP₃ generation) in tandem with extracellular Ca²⁺ influx^{24,25}. Indeed, blocking intracellular Ca²⁺ uptake with 1-μM thapsigargin to deplete the Ca²⁺-release pool gradually eliminated the muscle's light response (Fig. 4c, top; 3 muscles). The muscle's resting tension increased and oscillated during thapsigargin application, suggesting poor intracellular Ca²⁺-handling. Removing extracellular Ca²⁺ likewise reduced the light response by ~80% (Fig 4c, bottom; see also Ref. 9, 10, 12) and partially relaxed the resting tension. Because membrane depolarization is reportedly unnecessary for the intrinsic PLR in lower vertebrates^{9,10}, Ca²⁺-permeable ion channels other than voltage-gated Ca channels are likely involved, with TRP channels – especially TRPC channels – being candidates²⁵. However, neither the

TRPC1/4/5 nor the TRPC3/6/7 subfamily was apparently involved because the *Trpc1,4,5*^{-/-} and *Trpc3,6,7*^{-/-} genotypes appeared normal (**Methods** and Supplementary Fig. S4b). A role of TRPV4 in smooth muscle has also been described²⁵, but the muscle from *Trpv4*^{-/-} mice²⁷ was also normal (**Methods** and Supplementary Fig. S4b). With the apparent complexity of Ca²⁺ release and Ca²⁺ influx of unknown proportions^{10,28}, we did not attempt to dissect the mechanistic details further.

Phototransduction pathway in ipRGCs

We carried out the same interrogation on single ipRGCs (**Methods**). We focused on the M1-subtype, ipRGCs with by far the highest photosensitivity and largest responses^{3,4}, and also strongly labeled in our *Opn4:tdTomato* BAC-transgenic line¹⁵. Indeed, dissociated *Plcβ4*^{-/-} *Opn4:tdTomato* M1-ipRGCs gave no detectable responses (Fig. 5a, left; 6 cells, 23°C). In flat-mount retina, *Plcβ4*^{-/-} ipRGCs (with normal impulse-firing upon current injection) showed a tiny saturated response (2.7 ± 2.8 pA, 4 cells) to strong flashes ($2.1\text{--}4.0 \times 10^9$ equivalent 480-nm photons μm^{-2}), or 1% of WT (Fig. 5a, right and Fig. 5c; 23°C). As with sphincter muscle, this small response may involve another PLCβ isoform or a minor pathway. Also, as with iris, U71322 did not block *in situ* WT M1-ipRGC responses in flat-mount retina (not shown; see also Ref. 29), presumably due again to poor drug penetration²⁹.

Interestingly, at 23°C for recording stability, M1-ipRGCs from *Trpc6,7*^{-/-} mice (crossed into *Opn4:tdTomato*¹⁵ for cell identification; **Methods**) were not intrinsically photosensitive (Fig. 5b, c). Single-KO *Trpc6*^{-/-} and *Trpc7*^{-/-} M1-ipRGCs had similar sensitivities and saturated photocurrents as WT, albeit with distinct response kinetics (Fig. 5b–d). TRPC6 and TRPC7 likely form heteromeric ion channels in ipRGCs, although separate homomeric channels are remotely still possible (Supplementary Fig. S6). The *Trpc1,4,5*^{-/-} and *Trpc3*^{-/-} phenotypes were both like WT (Fig. 5b–d), while *Trpc3,6*^{-/-} and *Trpc3,6,7*^{-/-} (5 cells each) resembled *Trpc6*^{-/-} and *Trpc6,7*^{-/-}, respectively (not shown). The TRPC-subfamily is the closest vertebrate homolog of *Drosophila* TRP/TRPL channels mediating rhabdomeric phototransduction downstream of NorpA³⁰.

At 35°C, M1-ipRGCs (further validated by intracellular dye-labeling after recordings; **Methods**) of *Trpc6,7*^{-/-} genotype did give detectable, albeit tiny, responses (1% of WT) to strong flashes ($1.1\text{--}1.9 \times 10^9$ equivalent 480-nm photons μm^{-2}), as did *Trpc3,6,7*^{-/-} cells (Supplementary Fig. S7). Presumably, these residual responses would be even smaller¹⁵ and undetectable at 23°C. *Opn4*^{-/-} cells, however, remained unresponsive at 35°C (Supplementary Fig. S7).

Functional contribution of intrinsic PLR in mouse

Because of the intrinsic PLR, the overall pupil constriction in an illuminated eye should be stronger than the consensual constriction in the contralateral, unilluminated eye. Accordingly, we simultaneously monitored both pupils of a mouse while subjecting one eye to Ganzfeld illumination (2-min light step; **Methods**). For WT animals, the intensity-response (I-R) relations for the ipsilateral and contralateral PLRs were identical at the

dimmer intensities but diverged thereafter, with the ipsilateral PLR indeed being always stronger within a given animal (Fig. 6a, b, top panel). For *Opn4*^{-/-} animals, some bilateral asymmetry persisted but it was noticeably smaller especially at high intensities, with both I-R relations being broadly similar to WT except for a lower maximal PLR as found previously¹⁸ (Fig. 6a, b, second panel from top). For mice lacking rod and cone signals¹⁵ (*Gnat1*^{-/-} *cl*), the I-R relation was shifted to much higher light-step intensities owing to exclusive signaling by melanopsin¹⁸, but the bilateral asymmetry at high intensities again became more obvious than *Opn4*^{-/-} (Fig. 6a, b, third panel from top). The residual asymmetry in *Opn4*^{-/-} may suggest slightly stronger rod/cone signals to the ipsilateral PLR as well, perhaps explaining some of the WT ipsi/contralateral disparity in PLR especially at lower intensities. Finally, *Gnat1*^{-/-} *cl* *Opn4*^{-/-} mice had practically no steady PLR (Ref. 31, but see Ref. 32) (Fig. 6a, b, bottom panel).

The above difference in bilateral asymmetry between WT and *Opn4*^{-/-} PLRs cannot distinguish between an intrinsic iridic PLR and a bilateral asymmetry in ipRGC signaling to the PLR because both mechanisms involve melanopsin. To isolate the intrinsic PLR, we eliminated retinal signaling from one eye in the WT mouse by transecting its optic nerve (**Methods**). When the denervated eye was illuminated (at >7 days postsurgery), the intact contralateral eye failed to respond as expected, whereas the PLR persisted in the denervated eye (Fig. 6c, right panel), with the action spectrum of melanopsin (Supplementary Fig. S8). This residual component is the isolated intrinsic PLR. Its I-R relation on the intensity axis (Fig. 6c, left panel) relative to that for the ipsilateral PLR of non-operated WT animals (Fig. 6a, top panel) indicates that the intrinsic PLR begins to contribute when the normal overall PLR is ~90% complete. Nonetheless, the intrinsic PLR even by itself would have been able to drive the pupillary constriction 80–90% to completion over ~2.5 log units of light-step intensities. Furthermore, the intrinsic PLR has, in reality, an even lower light threshold (thus contributing even more to the overall PLR) because its I-R relation shifted by ~1 log unit to lower intensities after topical application of TTX to the cornea (Fig. 6c, left panel), which blocked any tonic autonomic inputs to the dilator and sphincter muscles. In short, the intrinsic component participates in the highest ~3.5 log units of the overall ~9-log-unit dynamic range of light intensities spanned by the normal PLR in mouse, at least during 2 min of steady illumination.

To translate into natural conditions, the yellow-shaded region in Fig. 6c, left panel, spans approximately from laboratory light to outdoor daylight (**Methods**). We also directly simulated ambient light with white xenon-arc light (400–650 nm) of matched power (**Methods**). For example, in room light, an ipsilateral (i.e., intrinsic) PLR of 0.47 ± 0.10 fractional constriction was elicited from the denervated eye of WT mice (Fig. 6d, 5 animals), versus 0.89 ± 0.02 when ipRGCs were also active (*Gnat1*^{-/-} *cl* mice without transected optic nerve) (Fig. 6d, 6 animals). Thus, the intrinsic PLR contributes substantially to the melanopsin component of the overall PLR even in room light. Finally, exposing the bilaterally-denervated eyes of a dark-adapted mouse to genuine room or outdoor light indeed led to intrinsic PLRs of extents expected from above (not shown).

Similar denervation experiments on rhesus and owl monkeys revealed no intrinsic PLR (2 animals each; Supplementary Text), consistent with the above negative findings from their

sphincter muscles and with clinical observations from human patients presenting complete unilateral optic neuropathy (resulting in loss of photosensitivity in the affected eye) (Supplementary Text).

Discussion

We have discovered a surprising, widespread intrinsic PLR among non-primate mammals, with a strong positive correlation between a nocturnal/nocturnal-leaning habitat and an intrinsic PLR. Teleologically, an intrinsic PLR benefits such mammals (with highly-photosensitive, rod-dominant retinas more susceptible to photodamage³³) by sustaining a pupil constriction under strong steady light – a situation otherwise difficult to achieve with neural circuitry alone because of the meager light admitted through the tiny pupil to the retina. The reason for the loss of this feature in primates despite melanopsin's continued presence in iris is unclear. Our work also reveals some bilateral asymmetry in the PLR of normal mouse (cf. 34, 35), which we now know to come partly from the intrinsic iridic photosensitivity in the higher-intensity range.

The intrinsic PLR is driven by melanopsin in mouse, probably also rat and hamster. By extension, the same presumably applies to other mammals showing an intrinsic PLR. As such, the function, if any, of the rhodopsin in mouse iris (see Results) is unknown. For amphibians and fish, the evidence for rhodopsin driving the intrinsic PLR was indefinite^{8,9} and probably should be re-examined given our present findings and melanopsin's presence in the eyes of amphibians (retina and iris)²² and fish (Ref. 36; Hsi-Wen Liao and K.-W.Y., unpublished). In chicken, the intrinsic PLR reportedly has an action spectrum with λ_{max} at <400 nm (Ref. 11; confirmed by us but not shown). This is interesting because chicken also has melanopsin in the retina and iris^{11,37}.

Because melanopsin is phylogenetically related to rhabdomeric opsins²², it is perhaps not surprising that its phototransduction mechanism employs a PLC pathway. Previously, clues from heterologous expressions^{38,39}, pharmacology, electrophysiology and/or immunohistochemistry on frog melanophores⁴⁰, native ipRGCs²⁹ and sub-vertebrate chordates^{41,42} have all implicated such a pathway. With gene-knockout mouse lines, we have now established this pathway more definitively and identified the signaling enzyme as PLC β 4, the closest homolog of *Drosophila* NorpA and the phospholipase C that mediates rhabdomeric phototransduction in fly. Although PLC β 4 is shared by iris and ipRGCs (at least the M1-subtype), the pathway diverges downstream. For M1-ipRGCs, the depolarizing light response results from the opening of presumably heteromeric channels formed predominantly by TRPC6 and TRPC7 (with potentially additional non-TRPC or non-critical TRPC subunits), gated possibly by phosphatidylinositol-4,5-bisphosphate, PIP₂ (Ref. 29). This makeup of the native channel agrees with indirect suggestions from immunohistochemical^{43,44} and RT-PCR⁴⁵ studies. For the sphincter muscle, however, TRPC3/6/7 or TRPC1/4/5 are apparently not involved in the light-induced contraction. An intracellular Ca²⁺ release is clearly important for the intrinsic PLR (see Results), but apparently not for the ipRGC light response²⁹.

We have not yet identified the G_q -species signaling between melanopsin and PLC β 4. However, conventional wisdom³⁰, pharmacological evidence²⁹, and *in vitro* biochemistry⁴⁶ suggest that it (they) should belong to the G_q -subfamily.

Finally, ordinary retinal ganglion cells (i.e., non-ipRGCs) become intrinsically photosensitive when transduced by virus to express melanopsin⁴⁷. Because PLC β 4 and TRPC6 are both expressed generally in RGCs^{48,29,43,44}, the same signaling pathway may well underlie this virus-induced intrinsic photosensitivity.

NOTE

After we had completed the experiments on ipRGCs, a paper appeared⁴⁹ reporting that the *Trpc3*^{-/-} and *Trpc7*^{-/-} single-KO genotypes showed no effect on the ipRGC's light response, while the *Trpc6*^{-/-} genotype showed a smaller light response than WT. These data are not in quantitative agreement with ours reported here. We attribute this difference to the use of whole-cell recording by the other group, a recording configuration that, from our experience, does not monitor the light response of ipRGCs with the same fidelity as the perforated-patch recording adopted by us.

Methods Summary

All experimental details are provided in Supplementary Information. The experimental procedures on animals followed the guidelines of the Animal Care and Use committee of the Johns Hopkins University School of Medicine. All indicated errors are standard errors of the mean (SEM).

Supplementary Material

Refer to Web version on PubMed Central for supplementary material.

Acknowledgments

We thank the following individuals for kindly providing knockout mouse lines (those with no indicated affiliation are all at Johns Hopkins School of Medicine): Drs. Michael Caterina (*Trpv4*^{-/-}), Janis Lem (Tufts University) (*Rho*^{-/-} and *Gnat1*^{-/-}), Jason C. Chen (Virginia Commonwealth University) (*Rho*^{-/-}), Jeremy Nathans (*cl*, also known as *cone-DTA*), Aziz Sancar (University of North Carolina at Chapel Hill) (*Cry1,2*^{-/-}) and Lutz Birnbaumer (US National Institute of Environmental Health Sciences) (*Trpc1*^{-/-}, *Trpc3*^{-/-} and *Trpc6*^{-/-}). We thank Drs. David Marshak (University of Texas Medical Center, Houston), Rudiger von der Heydt, Xiaoqing Wang, and Vivien Casagrande (Vanderbilt Medical School) for eyes from baboon, rhesus monkey, marmoset and bush baby, respectively, and Drs. Wei Li (US National Eye Institute), Ruifa Mi, Brian O'Rourke, Laurie Pipitone, Dawn Ruben, David Ryugo, Laura Smale (Michigan State University), and Gordon Tomaselli for eyes of the other animals. Experiments on bush baby were carried out in Dr. Vivien Casagrande's laboratory with help and hospitality. We also thank Dr. Weidong Gao for suggestions on the force transducer, Drs. Fred Rieke (University of Washington at Seattle) and Alapakkam Sampath (University of Southern California) for suggestions on the design of the LED light system, Dr. Petri Ala-Laurila (University of Washington at Seattle) for the method of equivalent-480-nm-photon conversion, Dr. Hugh Cahill for the mouse-head-anchoring method, Dr. Xiaozhi Ren for help on western blots, Dr. Ofelia Garalde and Austin Chen for help in the monkey experiments, and Wendy W.S. Yue for help on RT-PCR. We also thank Terry Shelley for fabricating all custom equipment, Sue Kulason for help in data analysis, and Liusong Ding for mouse-genotyping support. Members of the Yau laboratory provided comments on the manuscript. This work was supported by U.S. NIH Grant EY14596 and the António Champalimaud Vision Award (Portugal) to K.-W.Y.

References

1. Berson DM, Dunn FA, Takao M. Phototransduction by retinal ganglion cells that set the circadian clock. *Science*. 2002; 295:1070–1073. [PubMed: 11834835]
2. Hattar S, Liao HW, Takao M, Berson DM, Yau KW. Melanopsin-containing retinal ganglion cells: architecture, projections, and intrinsic photosensitivity. *Science*. 2002; 295:1065–1070. [PubMed: 11834834]
3. Bailes HJ, Lucas RJ. Melanopsin and inner retinal photoreception. *Cell Mol Life Sci*. 2010; 67:99–111. [PubMed: 19865798]
4. Do MTH, Yau KW. Intrinsically photosensitive retinal ganglion cells. *Physiol Rev*. 2010; 90:1547–1581. [PubMed: 20959623]
5. Hankins MW, Peirson SN, Foster RG. Melanopsin: an exciting photopigment. *Trends Neurosci*. 2008; 31:27–36. [PubMed: 18054803]
6. Nayak SK, Jegla T, Panda S. Role of a novel photopigment, melanopsin, in behavioral adaptation to light. *Cell Mol Life Sci*. 2007; 64:144–154. [PubMed: 17160354]
7. Barr L. Photomechanical coupling in the vertebrate sphincter papillae. *Crit Rev Neurobiol*. 1989; 4:325–366. [PubMed: 2655940]
8. Seliger HH. Direct action of light in naturally pigmented muscle fibers. I. Action spectrum for contraction in eel iris sphincter. *J Gen Physiol*. 1962; 46:333–342. [PubMed: 13992712]
9. Barr L, Alpern M. Photosensitivity of the frog iris. *J Gen Physiol*. 1963; 46:1249–1265. [PubMed: 14043001]
10. Kargacin GJ, Detwiler PB. Light-evoked contraction of the photosensitive iris of the frog. *J Neurosci*. 1985; 5:3081–3087. [PubMed: 3932607]
11. Tu DC, Batten ML, Palzewski K, Van Gelder RN. Nonvisual photoreception in the chick iris. *Science*. 2004; 306:129–131. [PubMed: 15459395]
12. Bito LZ, Turansky DG. Photoactivation of pupillary constriction in the isolated *in vitro* iris of a mammal (*Mesocricetus auratus*). *Comp Biochem Physiol*. 1975; 50A:407–413.
13. Lau KC, So KF, Campbell G, Lieberman AR. Pupillary constriction in response to light in rodents, which does not depend on central neural pathways. *J Neurolog Sci*. 1992; 113:70–79.
14. Oyster, CW. *The Human Eye: Structure and Function*. Sinauer; Sunderland, Mass: 1999.
15. Do MTH, Kang SH, Xue T, Zhong H, Liao HW, Bergles DE, Yau KW. Photon capture and signalling by melanopsin retinal ganglion cells. *Nature*. 2009; 457:281–287. [PubMed: 19118382]
16. Blanchong JA, McElhinny TL, Mahoney MM, Smale L. Nocturnal and diurnal rhythms in the unstriped Nile rat, *Arvicanthis niloticus*. *J Biol Rhythms*. 1999; 14:364–377. [PubMed: 10511004]
17. Govardovskii VI, Fyhrquist N, Reuter T, Kuzmin DG, Donner K. In search of the visual pigment template. *Vis Neurosci*. 2000; 17:509–528. [PubMed: 11016572]
18. Lucas RJ, Hattar S, Takao M, Berson DM, Foster RG, Yau K-W. Diminished pupillary light reflex at high irradiances in melanopsin-knockout mice. *Science*. 2003; 299:245–247. [PubMed: 12522249]
19. Lem J, Krasnoperova NV, Calvert PD, Kosaras B, Cameron DA, Nicolò M, Makino CL, Sidman RL. Morphological, physiological, and biochemical changes in rhodopsin knockout mice. *Proc Natl Acad Sci USA*. 1999; 96:736–741. [PubMed: 9892703]
20. Vitaterna MH, Selby CP, Todo T, Niwa H, Thompson C, Fruechte EM, Hitomi K, Thresher RJ, Ishikawa T, Miyazaki J, Takahashi JS, Sancar A. Differential regulation of mammalian period genes and circadian rhythmicity by cryptochromes 1 and 2. *Proc Natl Acad Sci USA*. 1999; 96:12114–12119. [PubMed: 10518585]
21. Ghosh S, Salvador-Silva M, Coca-Prados M. The bovine iris-ciliary epithelium expresses components of rod phototransduction. *Neurosci Lett*. 2004; 370:7–12. [PubMed: 15489008]
22. Provencio I, Jiang G, De Grip WJ, Hayes WP, Rollag MD. Melanopsin: An opsin in melanophores, brain, and eye. *Proc Natl Acad Sci USA*. 1998; 95:340–345. [PubMed: 9419377]
23. Yau KW, Hardie RC. Phototransduction motifs and variations. *Cell*. 2009; 139:246–264. [PubMed: 19837030]

24. Berridge MJ. Smooth muscle cell calcium activation mechanisms. *J Physiol.* 2008; 586:5047–5061. [PubMed: 18787034]
25. Gonzalez-Cobos JC, Trebak M. TRPC channels in smooth muscle cells. *Front Biosci.* 2010; 15:1023–1039.
26. Jiang H, Lyubarsky A, Dodd R, Vardi N, Pugh E, Baylor DA, Simon MI, Wu D. Phospholipase C beta 4 is involved in modulating the visual response in mice. *Proc Natl Acad Sci USA.* 1996; 93:14598–14601. [PubMed: 8962098]
27. Suzuki M, Mizuno A, Kodaira K, Imai M. Impaired pressure sensation in mice lacking TRPV4. *J Biol Chem.* 2003; 278:22664–22668. [PubMed: 12692122]
28. Zucker R, Nolte J. Light-induced calcium release in a photosensitive vertebrate smooth muscle. *Nature.* 1978; 274:78–80. [PubMed: 662000]
29. Graham DM, Wong KY, Shapiro P, Frederick C, Pattabiraman K, Berson DM. Melanopsin ganglion cells use a membrane-associated rhabdomic phototransduction cascade. *J Neurophysiol.* 2008; 99:2522–2532. [PubMed: 18305089]
30. Venkatachalam K, Montell C. TRP channels. *Annu Rev Biochem.* 2007; 76:387–417. [PubMed: 17579562]
31. Hattar S, Lucas RJ, Mrosovsky N, Thompson S, Douglas RH, Hankins MW, Lem J, Biel M, Hofmann F, Foster RG, Yau KW. Melanopsin and rod-cone photoreceptive systems account for all major accessory visual functions in mice. *Nature.* 2003; 424:76–81. [PubMed: 12808468]
32. Allen AE, Cameron MA, Brown TM, Vugler AA, Lucas RJ. Visual responses in mice lacking critical components of all known retinal phototransduction cascades. *PLoS One.* 2010; 5(11):e15063. [PubMed: 21124780]
33. Organisciak DT, Vaughan DK. Retinal light damage: Mechanisms and protection. *Prog Retin Eye Res.* 2010; 29:113–134. [PubMed: 19951742]
34. Grozdanic S, Betts DM, Allbaugh RA, Sakaguchi DS, Kwon YH, Kardon RH, Sonea IM. Characterization of the pupil light reflex, electroretinogram and tonometric parameters in healthy mouse eyes. *Curr Eye Res.* 2003; 26:371–378. [PubMed: 12868018]
35. Zhu Y, Tu DC, Denner D, Shane T, Fitzgerald CM, Van Gelder RN. Melanopsin-dependent persistence and photopotential of murine pupillary light responses. *Invest Ophthalmol Vis Sci.* 2007; 48:1268–1275. [PubMed: 17325172]
36. Bellingham J, Whitmore D, Philp AR, Wells DJ, Foster RG. Zebrafish melanopsin: isolation, tissue localisation and phylogenetic position. *Brain Res Mol Brain Res.* 2002; 107:128–136. [PubMed: 12487121]
37. Chaurasia SS, Rollag MD, Jiang G, Hayes WP, Haque R, Natesan A, Zatz M, Tosini G, Liu C, Korf HW, Iuvone PM, Provencio I. Molecular cloning, localization and circadian expression of chicken melanopsin (Opn4): differential regulation of expression in pineal and retinal cell types. *J Neurochem.* 2005; 92:158–170. [PubMed: 15606905]
38. Panda S, Nayak SK, Campo B, Walker JR, Hogenesch JB, Jegla T. Illumination of the melanopsin signaling pathway. *Science.* 2005; 307:600–604. [PubMed: 15681390]
39. Qiu X, Kumbalasiri T, Carlson SM, Wong KY, Krishna V, Provencio I, Berson DM. Induction of photosensitivity by heterologous expression of melanopsin. *Nature.* 2005; 433:745–749. [PubMed: 15674243]
40. Isoldi MC, Rollag MD, Castrucci AM, Provencio I. Rhabdomic phototransduction initiated by the vertebrate photopigment melanopsin. *Proc Natl Acad Sci USA.* 2005; 102:1217–1221. [PubMed: 15653769]
41. Gomez M, del P, Angueyra JM, Nasi E. Light-transduction in melanopsin-expressing photoreceptors of *Amphioxus*. *Proc Natl Acad Sci USA.* 2009; 106:9081–9086. [PubMed: 19451628]
42. Koyanagi M, Kubokawa K, Tsukamoto H, Shichida Y, Terakita A. Cephalochordate melanopsin: evolutionary linkage between invertebrate visual cells and vertebrate photosensitive retinal ganglion cells. *Curr Biol.* 2005; 15:1065–1069. [PubMed: 15936279]
43. Warren EJ, Allen CN, Brown RL, Robinson DW. The light-activated signaling pathway in SCN-projecting rat retinal ganglion cells. *Eur J Neurosci.* 2006; 23:2477–2487. [PubMed: 16706854]

44. Sekaran S, Lall GS, Ralphs KL, Wolstenholme AJ, Lucas RJ, Foster RG, Hankins MW. 2-Aminoethoxydiphenylborane is an acute inhibitor of directly photosensitive retinal ganglion cell activity in vitro and in vivo. *J Neurosci.* 2007; 27:3981–3986. [PubMed: 17428972]
45. Hartwick AT, Bramley JR, Yu J, Stevens KT, Allen CN, Baldrige WH, Sollars PJ, Pickard GE. Light-evoked calcium responses of isolated melanopsin-expressing retinal ganglion cells. *J Neurosci.* 2007; 27:13468–13480. [PubMed: 18057205]
46. Terakita A, Tsukamoto H, Koyanagi M, Sugahara M, Yamashita T, Shichida Y. Expression and comparative characterization of Gq-coupled invertebrate visual pigments and melanopsin. *J Neurochem.* 2008; 105:883–890. [PubMed: 18088357]
47. Lin B, Koizumi A, Tanaka N, Panda S, Masland RH. Restoration of visual function in retinal degeneration mice by ectopic expression of melanopsin. *Proc Natl Acad Sci USA.* 2008; 105:16009–16014. [PubMed: 18836071]
48. Peng YW, Rhee SG, Yu WP, Ho YK, Schoen T, Chader GJ, Yau KW. Identification of components of a phosphoinositide signaling pathway in retinal rod outer segments. *Proc Natl Acad Sci USA.* 1997; 94:1995–2000. [PubMed: 9050893]
49. Perez-Leighton CE, Schmidt TM, Abramowitz J, Birnbaumer L, Kofuji P. Intrinsic phototransduction persists in melanopsin-expressing ganglion cells lacking diacylglycerol-sensitive TRPC subunits. *Eur J Neurosci.* 2011; 33:856–867. [PubMed: 21261756]
50. Cahill H, Nathans J. The optokinetic reflex as a tool for quantitative analyses of nervous system function in mice: application to genetic and drug-induced variation. *PLoS One.* 2008; 3(4):e2055. [PubMed: 18446207]

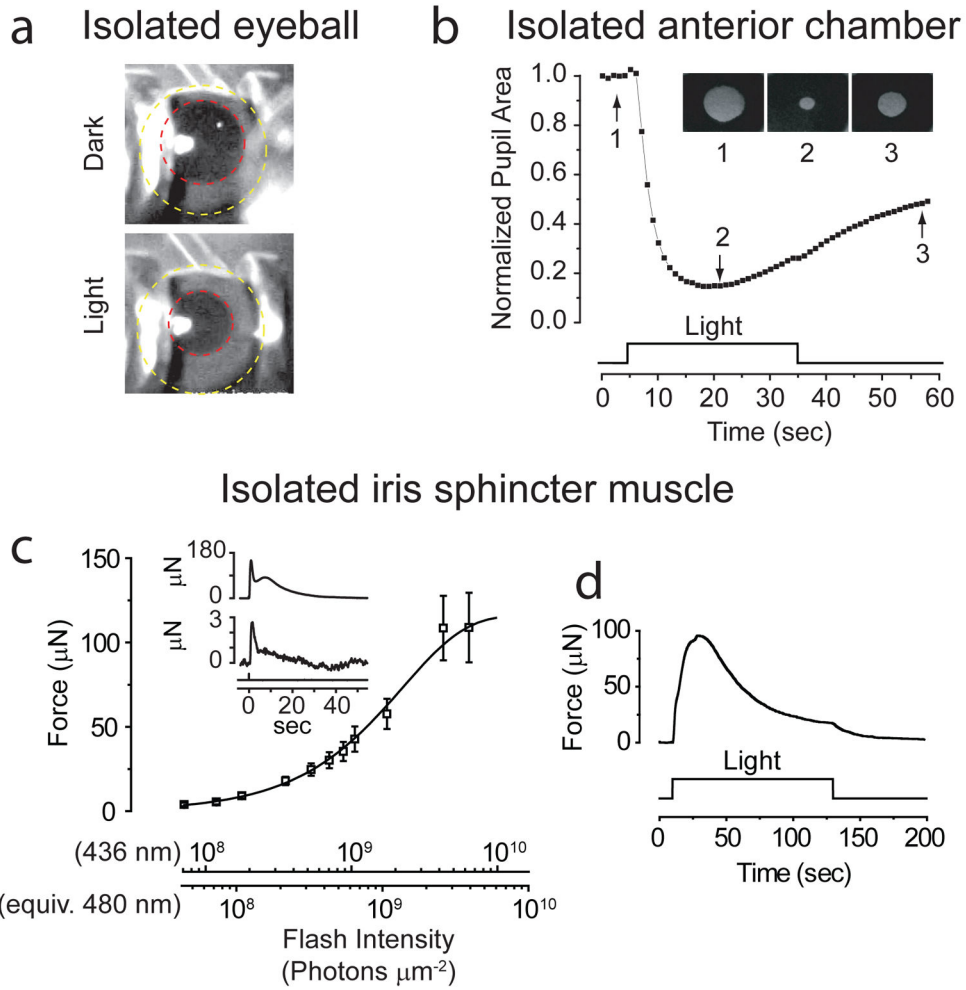


Figure 1. Intrinsic pupillary light reflex (PLR) of mouse. **a**, Constriction of pupil (red circle) in freshly isolated eye (yellow circle), elicited by $1.2 \times 10^{-3} \mu\text{W} \mu\text{m}^{-2}$ of white Xe light for ~ 3 sec over iris. 23°C . **b**, Intrinsic PLR in isolated anterior chamber, plotted as pupil area normalized to dark state. 23°C . *Inset* shows pupil at times indicated by arrows. White Xe light (30 sec of $4 \times 10^{-4} \mu\text{W} \mu\text{m}^{-2}$) over entire iris. **c**, Flash intensity-response relation for sphincter-muscle force at transient peak of response (mean \pm SEM, 7 muscles). $35\text{--}37^\circ\text{C}$. Fit is $R_{\text{max}}(1 - e^{-I/I_0})$ with $R_{\text{max}} = 116 \mu\text{N}$, $I_0 = 2.3 \times 10^9$ photons μm^{-2} (436-nm Hg light except for brightest two intensities, which were white; 3-mm spot covering entire muscle). Flashes were 12–400 ms in duration. *Inset* shows sample responses to a dim and a bright flash delivering (at time 0) 7.2×10^7 and 6.5×10^9 photons μm^{-2} (436 nm), respectively. **d**, Muscle-force response to a light step (6.1×10^9 photons $\mu\text{m}^{-2} \text{s}^{-1}$ at 436 nm) to indicate adaptation. Flash intensities are also expressed in equivalent 480-nm photons, given that melanopsin is the signaling pigment (see Fig. 3). All WT mice here and in subsequent figures were C57BL/6J, unless indicated otherwise.

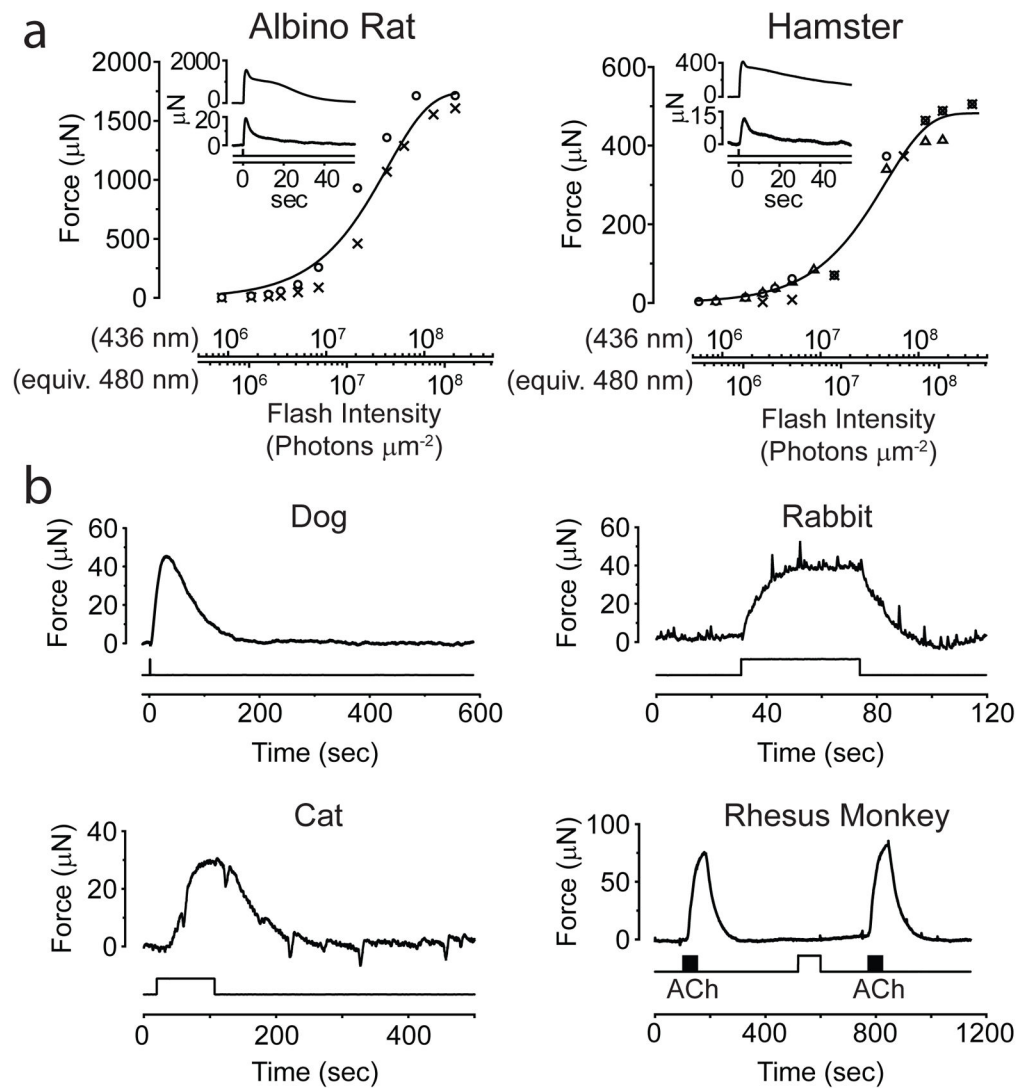
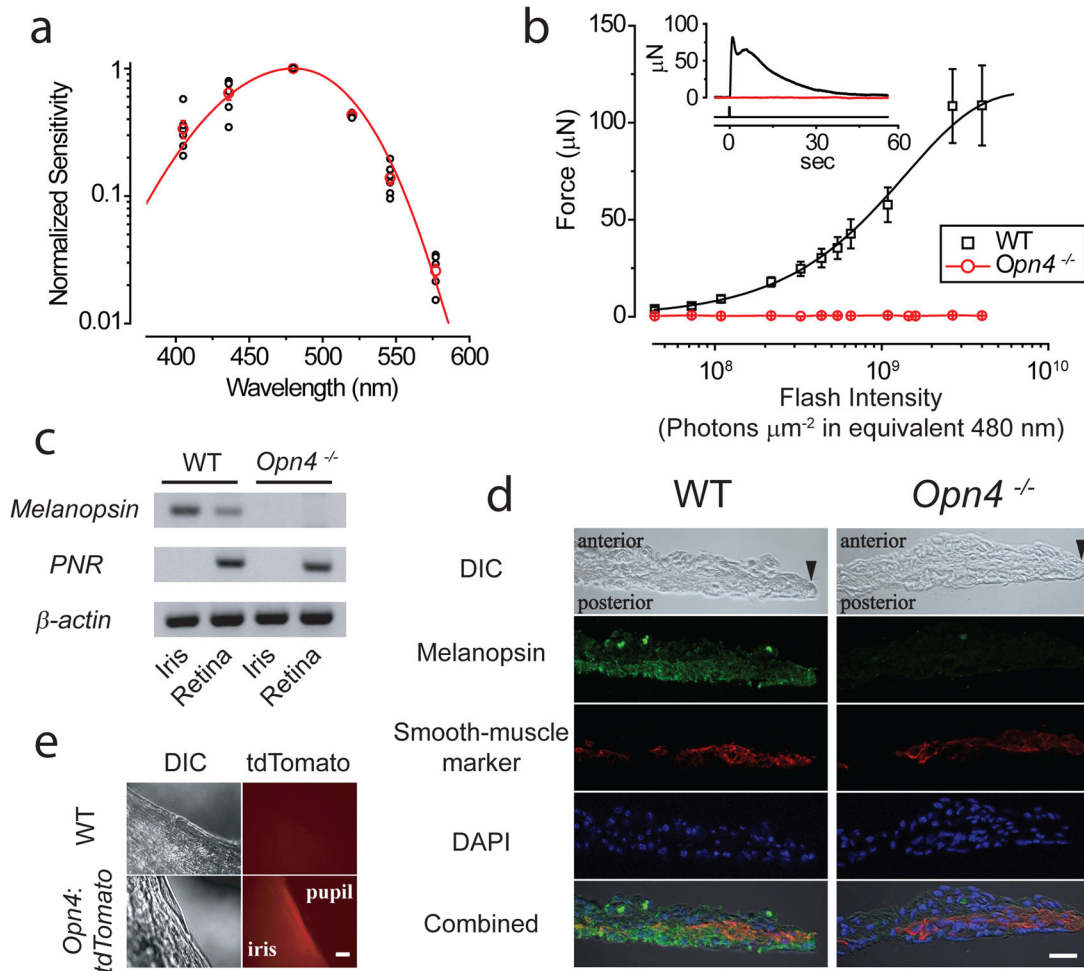


Figure 2. Intrinsic photosensitivity of iris sphincter muscle of other mammals. 35–37°C. **a**, Flash intensity-response relations from robust light responses of albino rat and pigmented hamster muscles (2 for rat and 3 for hamster). Same fits as in Fig. 1, with I_0 (averaged across individual muscles) being 4.3×10^7 photons μm^{-2} and 4.6×10^7 photons μm^{-2} (436 nm) for rat and hamster, respectively. Flashes were 12–400 ms. *Insets* show sample responses from a muscle of each species to dim and saturating flashes. 3.4×10^6 and 2.1×10^8 photons μm^{-2} for rat and 1.6×10^6 and 3.6×10^8 photons μm^{-2} for hamster, respectively (436-nm Hg light). **b**, Similar experiments on dog (representative of 2 muscles), rabbit (3), cat (1) and rhesus monkey (7). All steps and the flash (600-ms) delivered 6.1×10^9 photons $\mu\text{m}^{-2} \text{s}^{-1}$ (436-nm). Monkey muscle (pre-incubated with 30- μM 9-*cis*-retinal for 1 hr) gave no obvious light response, but responded to 50- μM acetylcholine in bath (black bars). Fast deflections in the rabbit and cat experiments reflected spontaneous muscle contractions/relaxations of unknown cause. 5-mm-diameter light spot, covering entire muscle of rat, hamster, cat and rabbit, but only partially the larger muscles of others.

**Figure 3.**

Dependence of intrinsic PLR on melanopsin. **a**, Action spectrum of mouse muscle (WT pigmented) (6 muscles), with sensitivity normalized to value at 480 nm in each experiment. Red circles are averages, and curve is an A_1 -pigment spectral template¹⁷ with $\lambda_{\text{max}} = 480\text{nm}$. Hg light with interference filters used. **b**, Average flash intensity-response relation for *Opn4*^{-/-} muscle (3 muscles). WT relation from Fig. 1c also shown for comparison. *Inset* shows sample responses of WT and *Opn4*^{-/-} muscles to a saturating flash of 4.0×10^9 photons μm^{-2} (equivalent 480 nm). **c**, Melanopsin (*Opn4*) mRNA detected by RT-PCR in iris and retina from WT but not *Opn4*^{-/-}. *PNR* (photoreceptor-specific nuclear receptor) mRNA used as control to rule out contamination from retina to iris. β -actin mRNA is a positive control. Difference in melanopsin mRNA signal between iris and retina presumably reflects different fractional total-tissue mRNA coding for melanopsin. **d**, Immunostaining of WT and *Opn4*^{-/-} iris cross-sections for melanopsin (green), smooth-muscle α -actin (red, as muscle marker), and DAPI (blue). Anterior side (stroma) up and posterior side (posterior epithelium) down. Black arrowhead marks pupillary edge. The intensity of melanopsin immunofluorescence appeared lower in the iris than in ipRGCs (not shown). Additionally, although the *Opn4*^{-/-} mouse contains the *tau-lacZ* marker gene replacing *Opn4*¹⁸, β -galactosidase activity (by X-gal labeling) was not evident in the iris (not shown),

presumably due to the low melanopsin-promoter activity. Scale bar: 20 μm . **e**, TdTomato signal detected in iris of *Opn4:tdTomato* but not WT mouse. Scale bar: 100 μm . Stimuli in **b** were 436-nm Hg light, and white for the two brightest intensities, although expressed in equivalent 480-nm photons. 3-mm-diameter spot covering entire muscle. All force measurements at 35–37°C. Mice in **d** and **e** were albino (C57BL/6J-Tyr^{c-2J}/J).

Author Manuscript

Author Manuscript

Author Manuscript

Author Manuscript

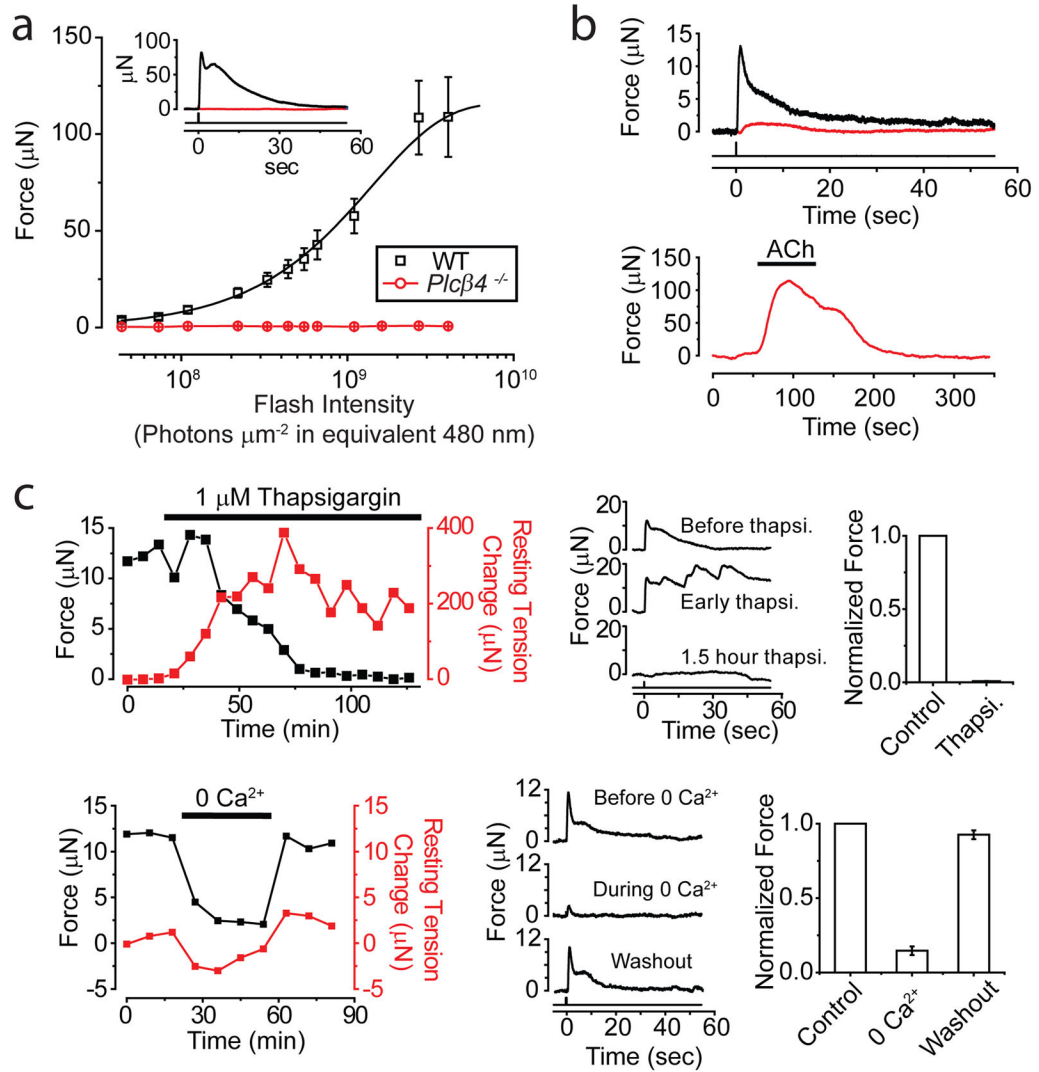


Figure 4.

Phototransduction mechanism underlying intrinsic PLR. **a**, Average flash intensity-response relation for *Plcβ4*^{-/-} muscle (5 experiments). WT relation from Fig. 1c shown for comparison. *Inset* shows sample responses of WT and *Plcβ4*^{-/-} to a saturating flash, at 4.0×10^9 photons μm^{-2} (equivalent 480 nm). **b**, *Top*, Example of a *Plcβ4*^{-/-} muscle (red) showing a tiny response ($<3 \mu\text{N}$) to first few dim flashes (7.3×10^7 photons μm^{-2}) before becoming unresponsive. WT response (black) to same dim stimulus also shown for comparison. *Bottom*, Same *Plcβ4*^{-/-} muscle nonetheless responded substantially to 10- μM acetylcholine. **c**, Thapsigargin and removal of extracellular Ca^{2+} , respectively, greatly diminished light response. *Left*, Time course of effect on peak force (black) generated by dim flashes (1.1×10^8 photons μm^{-2}). Resting muscle tension (red) arbitrarily set as 0 before thapsigargin or 0- Ca^{2+} application. *Middle*, Sample responses. *Right*, Collected data (4 muscles each). White Hg light for two brightest flashes in intensity-response relations of **a**; all other stimuli were 436-nm Hg light. All intensities expressed in equivalent 480 nm

photons. Flashes delivered at time 0, as a 3-mm-diameter spot covering entire muscle. 35–37°C.

Author Manuscript

Author Manuscript

Author Manuscript

Author Manuscript

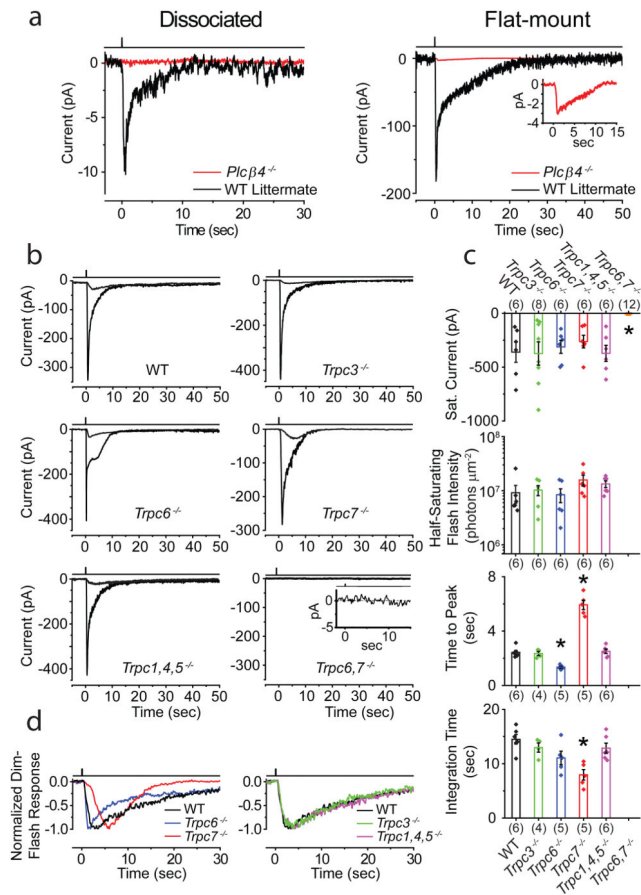


Figure 5.

Phototransduction mechanism and components underlying ipRGC intrinsic light response. Cells identified for electrical recordings based on *Opn4:tdTomato* reporter background in all mouse lines. 23°C. **a, Left**, Dissociated *Plcβ4*^{-/-} ipRGCs showed no detectable response to a saturating white Xe flash. Average of 4 trials for each response. **Right**, In flat-mount retina after synaptic block, *Plcβ4*^{-/-} ipRGCs showed a tiny residual response (magnified in *inset*) to similar saturating flash. Single flash trial for WT-littermate, and average of 5 trials for *Plcβ4*^{-/-}, explaining the low baseline noise in latter. 50–100 ms flashes delivering $1.97 - 3.94 \times 10^9$ photons μm^{-2} (equivalent 480 nm) in all cases. **b**, Intrinsic light responses from ipRGCs in flat-mount retina from WT, *Trpc3*^{-/-}, *Trpc6*^{-/-}, *Trpc7*^{-/-}, *Trpc1,4,5*^{-/-} and *Trpc6,7*^{-/-} mice. Averaged responses to both dim ($2.28-7.76 \times 10^5$ photons μm^{-2}) and saturating flashes (2.05×10^8 photons μm^{-2}) in each case are shown except *Trpc6,7*^{-/-}, for which only response to brightest flash is shown (magnified in *inset* and essentially zero). Flashes were 100–300 ms of 505-nm LED light. **c**, Comparison of saturated response amplitude and dim-flash-response parameters from **b**. Half-saturating flash intensity (i.e., intensity eliciting a half-maximum response) is inversely proportional to sensitivity. Time-to-peak is the time lapse between flash and transient peak of dim-flash response. Integration time, t_i , of the dim-flash response is a measure of its overall duration, given by $t_i = \int f(t)dt/f_p$, where $f(t)$ is response profile and f_p is its transient-peak amplitude. Collected data (mean \pm SEM), where “*” indicates $p < 0.001$ compared to WT by two-samples t-test. The

number of cells examined for each parameter is in parentheses, and not always the same across parameters because not all parameters were obtainable for each cell. **d**, Normalized, averaged dim-flash responses from **b** for comparison of response waveforms. All intensities expressed in equivalent 480-nm photons, and delivered as a 730- μm -diameter spot centered on soma, sufficient for covering entire intact cell in retina. Light monitor above each trace. All recordings in perforated-patch, voltage-clamp mode ($V_{\text{hold}} = -80 \text{ mV}$), with synaptic transmission blocked pharmacologically.

Author Manuscript

Author Manuscript

Author Manuscript

Author Manuscript

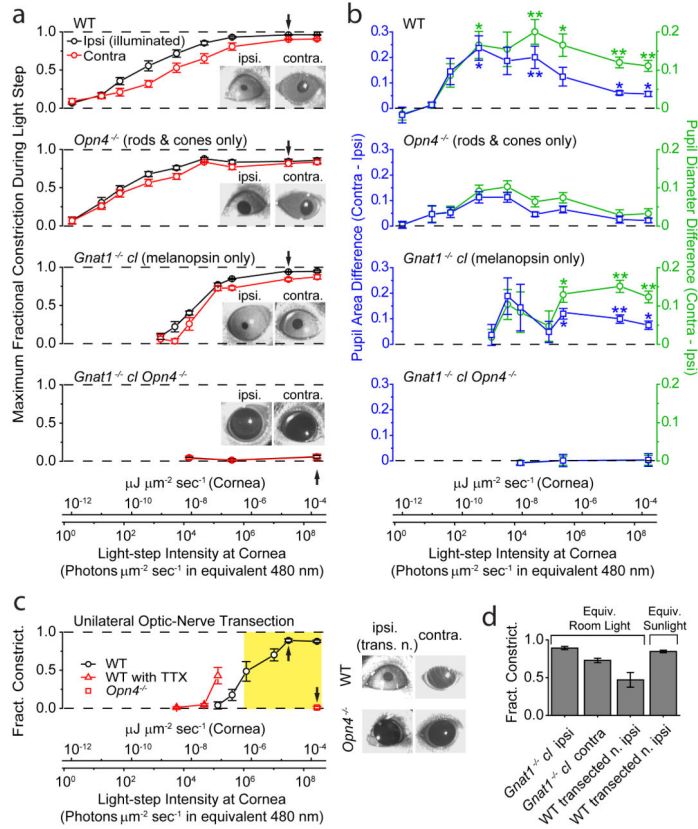


Figure 6. Simultaneous direct (ipsilateral) and consensual (contralateral) PLRs to unilateral illumination for different mouse genotypes *in situ*. 2-min of 505-nm LED light in **a-c**. PLR in ipsilateral, illuminated eye was measured at peak during this 2-min period, with contralateral PLR measured simultaneously. For **a** and **b**, conversion of light intensities into equivalent 480-nm photons applies strictly only to *Gnat1^{-/-} cl*, but not to WT or *Opn4^{-/-}* genotypes (which involved also rod/cone signals), because it required action spectrum of melanopsin. For this reason, light intensities are also given in the general unit of $\mu\text{J } \mu\text{m}^{-2} \text{ s}^{-1}$ (same as $\mu\text{W } \mu\text{m}^{-2}$). **a**, Average step intensity-response (I-R) relations for WT, *Opn4^{-/-}*, *Gnat1^{-/-} cl*, and *Gnat1^{-/-} cl Opn4^{-/-}* mice. PLR expressed as MFC (Maximum Fractional Constriction), where $\text{MFC} = 1 - (\text{Normalized Pupil Area in Light}) = 1 - (\text{Pupil Area in Light} / \text{Pupil Area in Darkness})$. *Inset* shows exemplary bilateral PLRs at an intensity indicated by arrow on I-R relations. Number of animals were 7 (WT), 7 (*Opn4^{-/-}*), 5 (*Gnat1^{-/-} cl*) and 3 (*Opn4^{-/-} Gnat1^{-/-} cl*). **b**, Ipsi/contralateral difference in normalized pupil area and diameter. For area, this difference is simply the difference between the ipsi- and contralateral values in **a**. For diameter, normalized diameter is $(\text{Normalized Area})^{1/2} = (1 - \text{MFC})^{1/2}$, calculable from data in **a**; the ipsi/contralateral difference values can then be evaluated (see **Methods** for significance of diameter). The area or diameter difference at a given intensity was then averaged over all animals of a given genotypic group. “**” indicates $p < 0.01$, and “*” indicates $p < 0.05$, when a WT or *Gnat1^{-/-} cl* value is compared to corresponding *Opn4^{-/-}* value by two-samples t-test. **c**, Direct (ipsilateral) PLR of eye with transected optic nerve to isolate the intrinsic component. WT mice in the absence or presence of TTX (5 μl of 600-

μM TTX in water administered on the cornea) (same set of 5 animals), and *Opn4*^{-/-} mice (4 animals). Images on right show exemplary bilateral PLRs (without TTX) at an intensity indicated by arrow on corresponding I-R relations. *Opn4*^{-/-} animals with transected optic nerve gave essentially no PLR. Yellow shaded area indicates light-intensity range from room light (with a minimum measured as $1.0 \times 10^{-6} \mu\text{W} \mu\text{m}^{-2}$, or 1.1×10^6 equivalent 480-nm photons $\mu\text{m}^{-2} \text{s}^{-1}$) to direct sunlight (measured as $3.7 \times 10^{-4} \mu\text{W} \mu\text{m}^{-2}$, or 3.9×10^8 equivalent 480-nm photons $\mu\text{m}^{-2} \text{s}^{-1}$) (**Methods**). **d**, Pupil constriction triggered by white light (400–650-nm bandpass filter; Xe lamp), matched in power to average common room light and ambient sunlight (**Methods**) (2.2×10^{-6} and $4.2 \times 10^{-5} \mu\text{W} \mu\text{m}^{-2}$, respectively), for *Gnat1*^{-/- cl} without optic-nerve transaction (6 animals) and WT mice with optic-nerve transaction (5 animals). All light rendered adirectional with Ganzfeld diffusing sphere. Pupils video-recorded under dim infrared light that did not activate any photoreceptors. All error bars are S.E.M.